Plasmonic Metasurfaces for the Near-Field Directional Control of Spontaneous Light Emission

Xiaowei Wang[1*], Yuyu Li[1], Reyhaneh Toufanian[2], Leonard C. Kogos[1], Allison Dennis[2], and Roberto Paiella[1]
[1] *Department of Electrical and Computer Engineering and Photonics Center, Boston University, 8 St. Mary's St., Boston, MA 02215, USA*
[2] *Division of Materials Science and Engineering, Boston University, 8 St. Mary's St., Boston, MA 02215, USA*
**Corresponding author: xwwang@bu.edu*

Abstract: We investigate the ability of gradient metasurfaces to promote directional light emission from an ensemble of dipole sources (colloidal quantum dots) in their near field. Well-collimated output beams along geometrically tunable directions are measured.

1. Introduction

Phase gradient metasurfaces (GMSs) have been widely investigated in recent years as a means to tailor the wavefronts of externally incident light for passive device applications [1, 2]. At the same time, their application in active optoelectronic devices such as light emitters is far less established. In this work, we explore their ability to control the radiation properties of a nearby continuous ensemble of randomly-oriented incoherent dipole sources via near-field interactions. As highlighted in recent theoretical work [3], when an oscillating dipole is placed in the near-field vicinity of a generic GMS featuring a linearly graded reflection phase profile, highly directional and polarized radiation can be obtained at an enhanced emission rate. The resulting direction of peak emission is determined by the reflection phase gradient, and therefore can be tuned by design by varying the GMS geometrical parameters.

In the present work, these ideas are demonstrated experimentally using a continuous distribution of colloidal quantum dots (QDs) deposited on a GMS consisting of a one-dimensional array of rectangular plasmonic NPs on a metal film, designed to introduce a linear phase profile upon reflection. The underlying radiation mechanism involves the near-field excitation of surface plasmon polaritons (SPPs) at the metal film, and their selective diffractive scattering by the GMS into well-collimated beams along predetermined geometrically tunable directions. Five different devices are developed, each providing directional light emission along a different target direction. These results underscore the ability of GMSs to efficiently extract light from the active material of a light-emitting device, and radiate it in a desired direction without the use of any external bulk optical elements. This capability is technologically significant for the continued miniaturization and large-scale integration of optoelectronic components. Additional beam shaping functionalities, similarly implemented directly at the source level, can also be envisioned with more complex designs of the same metasurface platform.

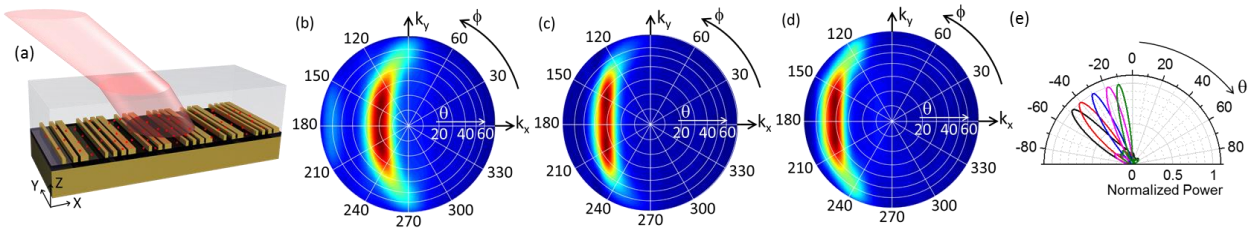

Fig. 1. (a) Schematic illustration of the device structure developed in this work, including its directional radiation output. (b)-(d) Calculated far-field radiation patterns of a planar ensemble of light-emitting dipoles near a GMS with polar angle of peak emission $\theta_0 = -20°$ (b), $-30°$ (c), and $-40°$ (d). In each color map, the radial distance from the origin corresponds to the polar emission angle θ, while the direction on the circle corresponds to the azimuthal angle ϕ. (e) Line cuts of all calculated radiation patterns along their horizontal axis normalized to their peak value.

2. Results and discussion

The specific GMS structure investigated in this work is illustrated in Fig. 1(a), where an array of rectangular Au NPs of fixed height (30 nm) is placed on a 30-nm-thick SiO_2 layer supported by an optically thick Au film. The array is capped with a polymer layer containing a planar ensemble of QDs [red dots in Fig. 1(a)]. The NP reflection phase (for *x*-polarized incident light at $\lambda = 800$ nm) can be tuned over a large fraction of the entire 2π phase space by varying its width L_x, while at the same time maintaining a relatively high reflection amplitude (> 78 %). A discretized version of the desired linear phase profile with gradient $\xi = 2\pi/\Lambda$ can then be implemented with a periodic array of period Λ, where each repeat unit contains N equally spaced NPs of different widths corresponding to equally spaced reflection-phase values across the full 2π range. A NP of zero width (i.e., a missing NP) is included in each unit cell, which is especially convenient from a fabrication standpoint. Additionally, in some devices two alternating unit cells with the

same length Λ but different numbers of NPs (N and N+1) are employed, as illustrated in Fig. 1(a). This arrangement allows for the complete suppression of spurious emission peaks at undesired angles, which would otherwise result from inadequate sampling of the target phase profile (unless exceedingly small inter-NP spacings are employed).

With this general approach, we have developed five different GMS structures designed to produce directional light emission peaked at different polar angles θ_0 in the free space above the polymer cap layer, ranging from –10° to –50° in steps of 10° (the negative signs here simply indicate that the in-plane wavevector of the output light is in the opposite direction relative to the GMS phase gradient). The radiation patterns of three representative devices computed by FDTD simulations are presented in Figs. 1(b)-(d), showing the expected tunable directional light emission. The characteristic C-shape of these patterns is consistent with the underlying radiation mechanism, where SPPs propagating along different directions on the Au plane are excited by the dipole sources and then scattered into radiation via positive-first-order diffraction by the GMS. The calculated 2D radiation patterns of all five devices developed in this work on the plane perpendicular to the NPs [the *x*-*z* plane of Fig. 1(a)] are shown in Fig. 1(e).

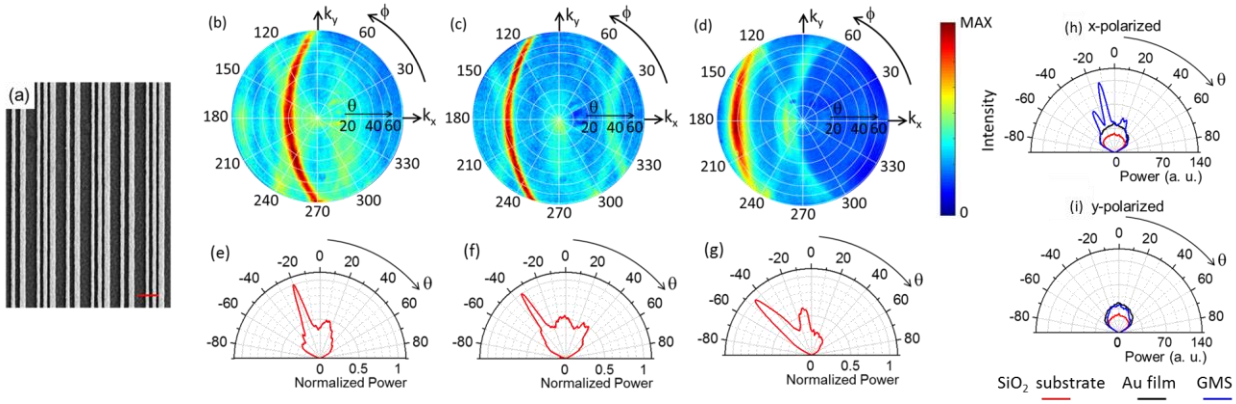

Fig. 2. (a) Top-view SEM image of a GMS designed for peak emission at $\theta_0 = -20°$. The scale bar is 500 nm. (b)-(g) Measurement results for three representative GMSs of different periods. (b)-(d) *X*-polarized far-field radiation patterns of a planar distribution of QDs in the near field of a GMS with θ_0 near –20° (b), –30° (c), –40° (d). (e)-(g) Line cuts of the color maps of (b)-(d) along their horizontal axis, rescaled by a cosθ normalization factor. (h)-(i) Comparison of the radiation patterns on the plane perpendicular to the NPs measured with identical QD ensembles on a GMS with $\theta_0 = -10°$ (blue trace), on the underlying Au film without any NP array (black trace), and on an uncoated substrate consisting of an oxidized Si wafer (red trace). Panels (h) and (i) show *x*- and *y*-polarized data, respectively.

Experimental samples are fabricated on Si/SiO_2 substrates using electron-beam lithography, and then planarized with a thin layer of spin-coated PMMA. CdTe/ZnS QDs suspended in a toluene/PLMA solution are then deposited by spin-casting, leading to a homogeneous distribution of randomly-oriented light emitters at a fixed distance (~ 15 nm) over the NPs. The resulting devices are finally capped with an optically thick (~ 10 μm) additional layer of PMMA. A top-view scanning electron microscopy (SEM) image of a 630-nm-period array is shown in Fig. 2(a). Figures 2(b)-(d) show the *x*-polarized far-field radiation patterns (at $\lambda = 800$ nm) measured with a Fourier microscopy setup from samples of target peak emission angles $\theta_0 = -20°$, –30°, and –40°. The expected C-shaped regions of high emission are clearly observed in these maps, with the corresponding line cuts along the horizontal axis [Figs. 2(e)-(g)] featuring a narrow beam with divergence angle (HWHM) as small as 5° in panel (f). The incomplete suppression of undesired diffraction orders observed in some of these plots is attributed to fabrication inaccuracies in the NP widths.

Finally, Figs. 2(h),(i) present a comparison of the *x*- and *y*-polarized radiation patterns measured with identical QD ensembles on a GMS (blue trace), on the underlying Au film without any NP array (black), and on a bare Si/SiO_2 substrate (red). An isotropic Lambertian profile is obtained from the two samples without the GMS and for the *y*-polarized emission from the GMS (also consistent with theoretical expectations). At the same time, significantly higher power is measured from the GMS device along its the target direction of peak emission, compared to the other two samples. The results presented in these plots therefore illustrate the ability of the GMSs under study to not only reshape the radiation pattern of nearby dipole sources, but also increase their radiation output through the same underlying near-field interactions.

This work was supported by NSF under Grant ECCS-1711156.

3. References

[1] N. Yu and F. Capasso, "Flat optics with designer metasurfaces," *Nature Mater.* **13**, 139 (2014).

[2] F. Ding, A. Pors, S. I. Bozhevolnyi, "Gradient metasurfaces: a review of fundamentals and applications," *Rep. Prog. Phys.* **81**, 026401 (2018).

[3] L. C. Kogos and R. Paiella, "Light emission near a gradient metasurface," *ACS Photon.* **3**, 243 (2016).